

Condensation of ablation plumes in the irradiation of metals by high-intensity nanosecond laser pulses at atmospheric pressure

K.V. Kozadaev

Abstract. The Anisimov–Luk’yanchuk model is adapted for describing the condensation of vapour-plasma plumes produced in the irradiation of metal targets by high-intensity (10^8 – 10^{10} W cm⁻²) nanosecond (10–100 ns) pulses at atmospheric pressure. The resultant data suggest that the initial stages of the development of metal ablation plumes correspond with a high degree of accuracy to the Zel’dovich–Raizer theory of dynamic condensation; however, at the stage of the ablation plume decay, the liquid-droplet phase is formed primarily by coalescence of ‘nuclei’.

Keywords: laser ablation, nanosecond laser pulse, Zel’dovich–Raizer theory, dynamic condensation, metal nanoparticles.

1. Introduction

The processes that take place in the laser erosion of metals have attracted the attention of researchers since the advent of lasers in the 60s of the past century [1–5]. The fundamental difficulty of describing the behaviour of a laser ablation plume arises from the strong nonuniformity and nonstationarity of this object, which are caused by the complex nature of the interaction of high-power laser radiation with a metal lattice. The physical picture of the laser erosion of metals is additionally complicated by the interaction of the plume with its generating radiation and by the possible effect of the ambient gases [1].

For sufficiently long laser pulses (longer than 1 μ s), the general physical picture of radiation interaction with metal targets has been rather well described theoretically [1–4] and verified experimentally [5–7] both for vacuum and for a broad range of pressure of extraneous gases. In this case, erosion processes are described by the ‘thermal’ model or the quasi-stationary ablation model, whereby relatively slow solid–liquid–vapour phase transitions take place in a metal under laser irradiation [1]. As this takes place, as a result of evaporation of the metal and gas-dynamic effects, ejection of target material (ablation) may occur in its vapour.

Shortening the duration of laser pulses to tens of or several nanoseconds for their relatively high intensity (10^8 – 10^{10} W cm⁻²) results in an interesting physical effect [8], when the rise time of a laser pulse approaches the characteristic electron–ion energy relaxation time in the metal lattice. To

state it in different terms, the rate of excitation energy input into the system, which consists of electron gas and lattice subsystems, becomes comparable with the highest rate of heat exchange between these subsystems. Therefore, the energy of laser radiation absorbed by conduction electrons does not have time to propagate into the target depth due to thermal conduction – the principal mechanism of energy transfer in the ‘thermal’ model. As a result, in the laser irradiation zone in the near-surface target region there forms a transition macroscopic layer, which possesses a substantial amount of excess energy (this is, in essence, a dense metal plasma) [1]. Owing to the detonation of the macrolayer, there occurs ejection of the target material (as in the previous case), this time due to different processes, which leads to qualitatively different physical effects. To describe these processes, use can be made of the ‘hydrodynamic’ model, or explosive ablation.

The main practical difficulty in using this model is determining the dynamics of the absorption coefficient for the incident laser radiation in dense metal plasma, with the consequence that the resultant plume may acquire additional energy. A consistent theory that models these effects has not been elaborated to date [9]. Nevertheless, S.I. Anisimov and B.S. Luk’yanchuk came up with a rather holistic model for describing the processes occurring in suchlike plumes upon completion of their formation (i.e. after termination of their interaction with the laser radiation). The model of Refs [9–12] relies on the assumption of the adiabatic expansion (in vacuum) of an axially or spherically symmetric vapour plasma cloud with parabolic or rectangular initial temperature and density profiles with the inclusion of dynamic condensation according to Zel’dovich–Raizer theory [13]. A comparison of the simulation data for Si, Ge and C plumes (with the initial conditions corresponding to the laser ablation of these material by high-intensity nanosecond pulses) with the experimental data of Ref. [14] revealed a good agreement between them even without adjustable parameters.

In this connection, a point of considerable practical interest is to adapt the Anisimov–Luk’yanchuk model to the case of laser erosion of metals by nanosecond pulses at atmospheric pressure. The presence of extraneous gases has a significant effect on the evolution and decay of such plumes; as a result, however, there also occurs condensation of the vapour plasma cloud and the formation of the nanodimensional dust phase of the target material [15–18]. Our present work is concerned with the development of a mathematical model for describing the expansion and condensation of laser ablation plumes of metals (produced under irradiation by high-intensity nanosecond pulses) at atmospheric pressure. In doing this we proceed from the analysis of existing experimental data and adapt the Anisimov–Luk’yanchuk model.

K.V. Kozadaev A.N. Sevchenko Institute of Applied Physical Problems, Belarussian State University, ul. Kurchatova 7, 220045 Minsk, Belarus; e-mail: kozadaeff@mail.ru

Received 10 March 2015
Kvantovaya Elektronika 46 (1) 16–22 (2015)
Translated by E.N. Ragozin

2. Vapour plasma cloud expansion

As discussed in the foregoing, from the practical standpoint it is expedient to begin the simulation of the ablation plume development from the point the plume ceases to interact with the incident laser radiation; this point in time corresponds to the beginning of free plume propagation without extraneous energy inflow. Experimentally, this instant corresponds to the attainment of the peak of a spectrum-integrated plume glow intensity at the peak of its heating by the radiation; as a rule, this instant occurs when the intensity of the irradiation laser pulse begins to decline [19]. For every specific metal the interval between the onset of laser irradiation and the instant of maximum plume temperature may somewhat vary, depending on the duration and intensity of the laser pulse. For instance, when a 20-ns-long pulse with an intensity of 10^8 – 10^9 W cm⁻² irradiates metals (Zn, Ni, Pb, Cu, Ag, Au), this interval is equal to 20–30 ns [18]. In this case, the spatial plume dimension may be determined by probing the plume at different heights above the target surface [20].

By way of illustration of the proposed approach, to verify the model in the present work we use experimental data on the laser erosion of lead by high-intensity nanosecond pulses at atmospheric pressure, which were obtained by the author and published in Refs [17–19].

In the Anisimov–Luk’yanchuk model, the following spherically symmetric model is proposed to describe the expansion of an ablation plume in vacuum [11, 9]:

$$\Psi(t) = \left(\frac{R(t)}{R_0}\right)^2 = 1 + 2\frac{u_0}{R_0}t + \left[\left(\frac{u_0}{R_0}\right)^2 + \frac{16E}{3MR_0^2}\right]t^2, \quad (1)$$

where $\Psi(t)$ is the dimensionless function which characterises the propagation dimension of the leading front of the spherical cloud; $R(t)$ is the radius of the spherical cloud; R_0 is the initial plume radius; u_0 is the initial velocity of plume propagation; E is the initial internal energy of the plume; and M is the mass of the plume vapour.

By analysing the available experimental data [17–19] it is possible to determine the initial parameters of the erosion plume required for this model. When a 20-ns-long pulse with an intensity of 10^9 W cm⁻² and a total pulse energy of 200 mJ irradiates a lead target, the initial radius of the hemispherical cloud which corresponds to the instant of highest temperature is $R_0 \approx 0.5$ mm, the initial velocity of the leading plume edge is $u_0 = 10$ km s⁻¹, and the average mass of the target material removed per pulse is $M = 10^{-8}$ kg. To estimate the initial internal energy of the vapour ($E = 2$ mJ), use was made of the data on the characteristic ablative loading of metals (the fraction of irradiation energy that goes into the kinetic plume energy) [21].

Curve (1) in Fig. 1a corresponds to the substitution of the initial parameters in formula (1). The experimental points were plotted using the data of Ref. [17]. One can see that the Anisimov–Luk’yanchuk approximation strongly overrates the plume dimensions in comparison with the experimental data (this comes as no surprise, considering that the model is intended to describe the plume expansion in vacuum). A far better result is provided by the spherically symmetric Taylor–Sedov model [22], which is employed to describe the front propagation for an explosion shock wave in buffer gases [Fig. 1, curve (2)]. This model exhibits a good agreement with the experimental points even without introducing adjustment coefficients (for the sake of pictorial clarity, the consistency of

experiment to the Taylor–Sedov model is shown both on a logarithmic scale, Fig. 1a, and on a linear scale, Fig. 1b):

$$\Psi(t) = \left(\frac{R(t)}{R_0}\right)^2 = \left[1 + \frac{\xi_0}{R_0} \left(\frac{E}{\rho_g}\right)^{1/5} t^{2/5}\right]^2, \quad (2)$$

where

$$\xi_0 = \left[\frac{75(\gamma_g - 1)(\gamma_g + 1)^2}{16\pi(3\gamma_g - 1)}\right]^{1/5} [13]; \quad (3)$$

ρ_g is the buffer gas density ($\rho_g = 0.029$ kg m⁻³ for the air); and γ_g is the adiabatic exponent of the buffer gas (for $\gamma_g = 7/5$, $\xi_0 = 1.014$). In this case, the expansion of the plume will be self-similar [13] up to the point it reaches the radius $r_0 = (E/p_g)^{1/3} \sim 3$ mm, where p_g is the buffer gas pressure.

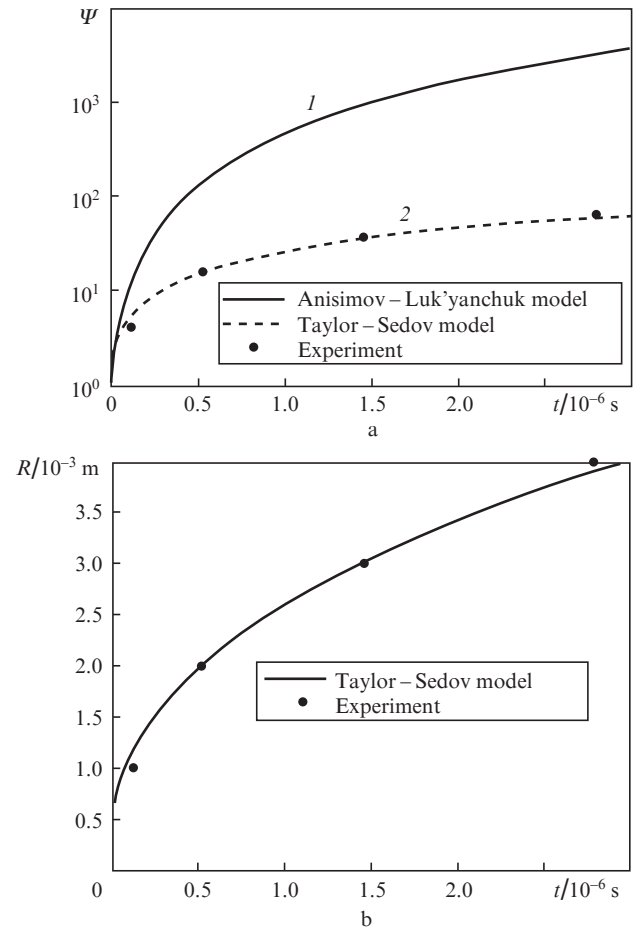


Figure 1. Dynamics of the leading edge boundary for a lead plume.

In the simulation of the temperature and density distributions of the gas inside the plume in the case of its adiabatic expansion in vacuum, Anisimov and Luk’yanchuk [9] and Arnold et al. [23] proposed the use of parabolic profiles with the parabola of degree two in order to match the parameters inside the plume to external parameters, and Kuwata et al. [12] adduced an example of employing rectangular profiles (i.e. the parameters are uniform over the plume). However, neither the former model nor the latter one provide adequate approximations in the case of a sufficiently dense external environment. The rectangular profile is *a fortiori* nonphysical owing to the infinitely abrupt transition from internal plume parameters to external ones, while a quadratic parabola pro-

vides too slow a decrease of the initial conditions (the dimension of the transition zone is much overestimated). That is why in the present work the relations from Ref. [9] that model the distributions of the gas temperature T_p (along the Poisson adiabat) and density inside the plume are adapted to the case when atmospheric gases are present by increasing the parabola degree to eight, which furnishes a more realistic size of the transition zone from internal parameters to external ones. Also added were the terms which provided correct boundary conditions (the temperature and density of the atmospheric gases at the external boundary of the plume):

$$T_p(r, t) = T_0(1 - \xi^8) \Psi(t)^{-1} + T_g \xi, \quad (4)$$

$$\rho(r, t) = \rho_0(1 - \xi^8)^{3/2} \Psi(t)^{-3/2} + \rho_g \xi, \quad (5)$$

where $\xi = r/R(t)$ is the dimensionless Lagrangian coordinate (inside the plume $0 \leq \xi \leq 1$); T_0 and ρ_0 are the initial vapour temperature and density at the plume centre; and $T_g \approx 300$ K is the buffer gas temperature.

The value of parameter T_0 may be determined by analysing the spectral structure of the glow of the peripheral region of the lead plume (under the indicated conditions) given in Ref. [19]. The maximum of the continuous spectrum of the

outer plume boundary glow at the moment the temperature is highest falls on a wavelength of 450 nm. From the Wien displacement law the temperature at the outer plume boundary is estimated at 6400 K, which in turn corresponds to $T_0 \approx 15000$ K. Knowing the mass and the radial vapour density distribution in the plume as well as the initial hemisphere radius R_0 , it is easy to estimate also the initial vapour density at the plume centre: $\rho_0 = 33M/(20\pi R_0^3) \approx 40$ kg m⁻³. The three-dimensional surfaces corresponding to the proposed spatio-temporal temperature distributions along the Poisson adiabat and the lead plume density are plotted in Fig. 2.

3. Condensation of ablation plume

In the adiabatic vapour expansion, condensation must necessarily set in at some point in time, according to Zel'dovich–Raizer theory [13]. This instant may be determined from the following considerations: in the phase state diagram, the vapour expansion proceeds along the Poisson adiabat until the instant of saturation (the intersection of the Poisson adiabat with the saturation adiabat defined by the Clausius–Clapeyron equation). Next, as the plume vapour continues to follow the Poisson adiabat, it becomes supersaturated (supercooled), and conditions are formed in it for the emergence of nucleation centres of the future droplets. The rate of condensation centre production depends exponentially on the degree of vapour supersaturation, which is defined by the supercooling parameter $\theta = (T_{eq} - T)/T_{eq}$, where T_{eq} is the temperature of thermodynamic equilibrium for the given vapour volume and pressure (the temperature along the vapour binodal). A sharp growth of θ is attended with a mass production of condensation centres ('injection' of nucleation centres), which begin to grow in size due to the adherence of vapour molecules. Due to the release of the latent condensation energy, the rapid droplet production in the vapour terminates the growth of the supercooling parameter and causes it to decrease. In this case, the nucleation centre production, which is highly sensitive to the degree of supersaturation, terminates and subsequently there occurs only the enlargement of the droplets produced. Because of the continuing rapid plume expansion, observed at this stage is a gradual decrease in the number of the events of adherence of vapour molecules to the nuclei and subsequently its complete termination. In this case, the degree x of vapour condensation (the ratio between the number of vapour atoms in the liquid phase to their total number) stabilises, which corresponds to the so-called droplet quenching. Therefore, unlike the 'equilibrium' static condensation scenario, when the vapour is in the state of thermodynamic equilibrium at all stages, in the case of rapid adiabatic plume expansion the highest attainable degree of condensation may be well below unity (0.1–0.3 in practice) [13].

The dynamic condensation of ablation plumes described above may be represented as the propagation, from the periphery to the centre through the expanding cloud, of three concentric shock waves: the saturation wave (which corresponds to the instant of intersection of the Poisson adiabat with the saturation adiabat in the phase diagram), the wave of nucleation centre 'injection' (the instant of greatest supercooling), and the 'quenching' wave (the stabilisation of the degree of plume condensation) [9, 10].

To consider the development of condensation in our work as well as in Refs [9–13], the liquid droplets produced in the course of plume expansion are assumed to travel together with the vapour (which is true for low degrees of its condensa-

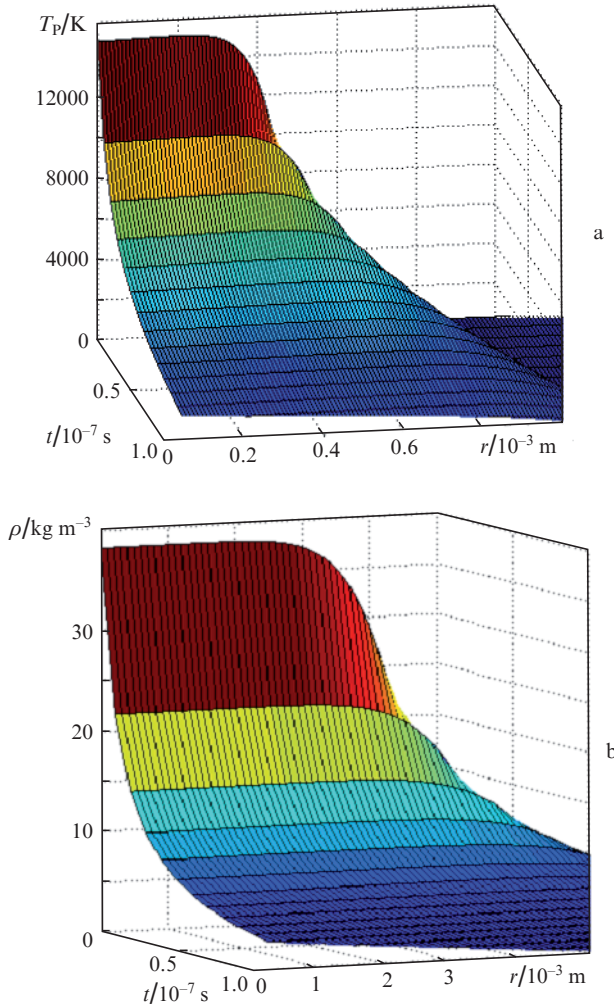


Figure 2. Spatiotemporal temperature distributions along the Poisson adiabat (a) and the density (b) of the lead plume.

tion). This assumption permits considering the condensation independently for every particle with a certain Lagrangian coordinate.

According to Ref. [9], the vapour temperature that corresponds to the onset of condensation (to the intersection of the Poisson adiabat with the saturation adiabat) is $T_c = q\Phi(a)$, where $q = Q/R_g$ is the specific heat of evaporation Q of the metal in Kelvin degrees; R_g is the universal gas constant; and $\Phi(a)$ is the lowest root of the transcendental equation [9]:

$$\Phi(a)\exp(\Phi(a)^{-1}) = \frac{B}{V_0} \left(\frac{q^2}{T_s T_0} \right)^{3/2}; \quad (6)$$

$B = R_g T_s / (\mu p_s)$; $V_0 = 1/\rho_0 = 0.025 \text{ m}^3 \text{ kg}^{-1}$ is the initial specific volume of the plume; $T_s = 300 \text{ K}$ is the normalisation temperature; μ is the molar mass of the metal (for lead, $\mu = 0.2 \text{ kg mol}^{-1}$); and p_s is the pre-exponential factor from Ref. [9] (for a specific metal it may be determined by approximating the data of Ref. [24], and $p_s = 10^{10} \text{ Pa}$ for lead). Upon substitution of the listed values in Eqn (6) and its numerical solution we find that $T_c = 2480 \text{ K}$.

The dynamics of thermodynamic equilibrium temperature $T_{\text{eq}}(t)$ (along the saturation adiabat) in the expanding plume may be determined by solving the transcendental functional equation [9]

$$V_0 \Psi(t)^{3/2} = [1 - x_{\text{eq}}(t)] B \left(\frac{T_{\text{eq}}(t)}{T_s} \right)^{3/2} \exp\left(\frac{q}{T_{\text{eq}}(t)}\right), \quad (7)$$

where

$$x_{\text{eq}}(t) = \frac{2q}{2q - T_{\text{eq}}(t)} \left(\frac{T_c - T_{\text{eq}}(t)}{T_c} + 3 \frac{T_{\text{eq}}(t)}{q} \ln \frac{T_{\text{eq}}(t)}{T_c} \right)$$

is the degree of condensation in the case of thermodynamic equilibrium in the vapour.

As discussed above, when the temperature $T_p(r, t)$ reaches a value T_c , there sets in an active droplet production, which is later attended with an intense liberation of the latent heat of condensation. This has the effect that the plume temperature departs from the Poisson adiabat and approaches the saturation adiabat. To determine the dynamics of the plume temperature T during this transition period, advantage can be taken of the relation for the local energy balance in a two-phase vapour–liquid system in the adiabatic approximation [13]:

$$[c_1(1-x) + c_2x]dT + R_g T(1-x) \frac{dV}{V}$$

$$- [Q - (c_2 - c_1)T]dx = 0, \quad (8)$$

where c_1 and c_2 are the vapour heat capacity at constant volume and the liquid heat capacity, respectively; and V is the specific volume of the vapour. Considering that $c_1 = 3R_g/2$ (in the ideal monoatomic gas approximation) and $dV/V = 3/2(d\Psi/\Psi)$, we may write the differential equation for the plume temperature, which takes into account the liberation of latent condensation energy:

$$(1 + \beta x(t)) \frac{dT(t)}{dt} + (1 - x(t)) \frac{T(t)}{\Psi(t)} \frac{d\Psi(t)}{dt} = \left(\frac{2}{3}q - \beta T(t) \right) \frac{dx(t)}{dt}, \quad (9)$$

where $\beta = (2c_2/3R_g) - 1$ ($\beta \approx 1.4$ for lead); $T(0) = T_p(t)|_{t=t_c} = T_c$; and t_c is the moment at which the vapour reaches the saturation temperature.

The plume temperature departs from the Poisson adiabat at the moment t_c of mass injection of nuclei, which corresponds the greatest supercooling of the vapour. This point in time can be found by solving the transcendental equation [9]

$$\frac{1}{T_{\text{eq}}(t)} \frac{dT_{\text{eq}}(t)}{dt} = - \frac{1}{\Psi(t)} \frac{d\Psi(t)}{dt} + \left(\frac{2q}{3T_p(t)} - 1 \right) \left(\frac{\alpha T_{\text{eq}}(t)}{T_{\text{eq}}(t) - T_p(t)} \right)^3 \times k_v \exp\left[- \frac{T_v}{T_p(t)(1 - T_p(t)/T_{\text{eq}}(t))^2} \right], \quad (10)$$

where

$$\alpha = \frac{2\sigma m}{k_B q \rho_{\text{liq}}} \left(\frac{4\pi \rho_{\text{liq}}}{3m} \right)^{1/3}; \quad T_v = \frac{16\pi \sigma^3 m^2}{k_B^3 q^2 \rho_{\text{liq}}^2}; \quad k_v = 4 \frac{\rho}{\rho_{\text{liq}}} \sqrt{\frac{2\sigma}{\pi m}};$$

σ is the force of surface tension; ρ_{liq} is the liquid phase density; k_B is the Boltzmann constant; and m is the atomic mass of the metal. In our case, $\alpha \approx 0.48$, $T_v \approx \text{K}$, and $k_v \approx 1.5 \times 10^{10}$.

For the solution of Eqn (9), the dynamics of the condensation degree $x(t)$ in the plume may be estimated from the relation

$$x(t) = \begin{cases} 0, & t_c < t < t_c, \\ x_{\text{eq}}(t - t_c), & t > t_c, \end{cases} \quad x(0) = x(t_c) = 0. \quad (11)$$

The time dependences of T , θ and x at the plume centre ($r = 0$), which were obtained in the numerical solution of Eqns (7), (9), and (10), are plotted in Fig. 3. This drawing provides

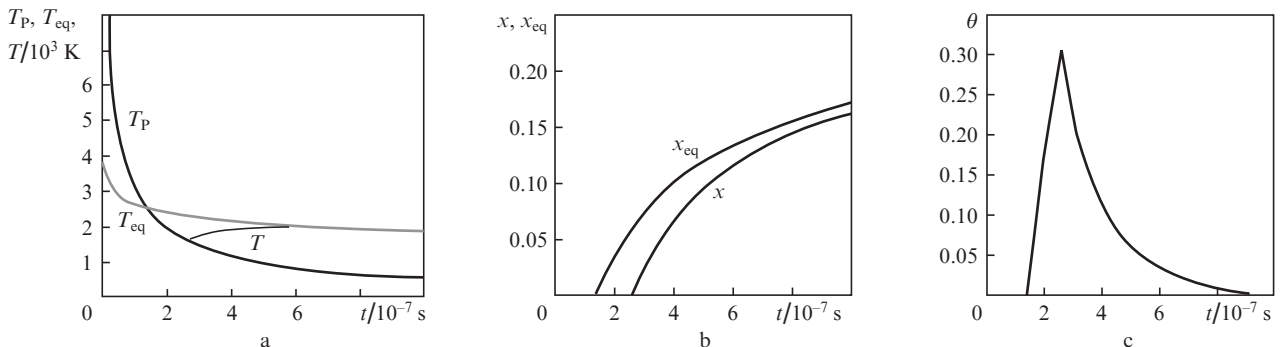


Figure 3. Time dependences of the simulated parameters at the plume centre ($r = 0$).

a good illustration of the features of condensation, which proceeds according to the Zel'dovich–Raizer theory (the effects of saturation and nuclei ‘injection’ [13]).

To estimate the spatiotemporal characteristics of the ‘quenching’ wave (which corresponds to the cessation of droplet formation), Luk’yanchuk et al. [10] proposed using the relation

$$\frac{r_q(t)}{R(t)} = \sqrt{1 - \left(t_k \Psi(t) \frac{d\Psi(t)}{dt} \right)^{1/2}}, \quad (12)$$

where

$$t_k = \frac{mV_0}{2\sigma_g} \sqrt{\frac{3m}{5k_B T_0}};$$

$r_q(t)$ is the radius of the ‘quenching’ wave; and σ_g is the collision cross section.

Figure 4 shows the trajectories of the saturation, ‘injection’ and ‘quenching’ waves, which were constructed proceeding from an analysis of the solutions of Eqns (6)–(12) in the interval 0–3 μ s.

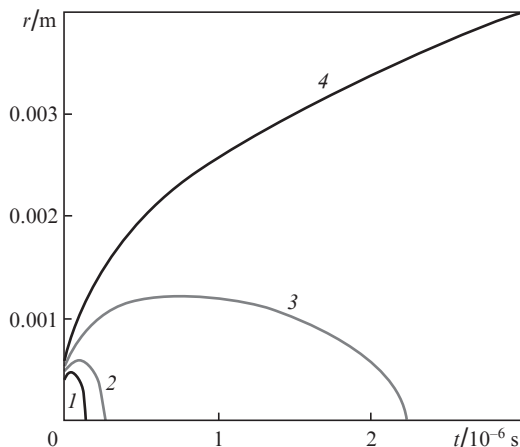


Figure 4. Trajectories of the saturation (1), ‘injection’ (2) and ‘quenching’ (3) waves, as well as the radius of the leading edge of the plume (4).

The model spatiotemporal scale of the ‘injection’ wave agrees nicely with the experimental probing data for such plumes obtained by Goncharov et al. [17]. This physical effect manifested itself in Ref. [17] in the emergence and rapid build-up of the scattered component in the interaction of the probe radiation with the plume, i.e. a large number of scattering centres did emerge in the probe zone at that point in time. The same is also true of the parameters of the model ‘quenching’ wave (when the droplets produced in the plume cease to grow): in the corresponding drawings in Ref. [17] they are characterised by the instants of stabilisation of the intensity behaviour of the scattered and absorbed components of the probe radiation in the plume, which set in 2–2.5 μ s after laser irradiation.

According to the Anisimov–Luk’yanchuk model, the kinetics of plume condensation is determined by the behaviour of the functions $x(t) = g(t)v(t)$ from the instant of nuclei ‘injection’ to the instant of their ‘quenching’ ($g(t)$ is the cluster-droplet dimension in terms of the number of atoms and $v(t)$ is the ratio between the number of nuclei and the total

number of vapour atoms). To model these functions, Anisimov and Luk’yanchuk [9] proposed solving the system of the corresponding ordinary differential equations subject to the initial conditions that correspond to the instant of greatest vapour supercooling. Luk’yanchuk et al. [10] considered an example of such numerical simulation for the expansion of Si, Ge and C ablation plumes ($T_0 = 7000$ – 8000 K, $V_0 = 200$ – 300 cm³ g⁻¹, $R_0 = 1$ mm, $u_0 = 6$ km s⁻¹ and $M = 0.3$ – $0.5 \cdot 10^{-9}$ kg) in vacuum. They showed, in particular, that the critical dimension of droplet nuclei (when the supercritical nuclei become immune to disintegration) is equal to 10–20 atoms of the corresponding substance. According to Refs [9, 10], the critical nucleus size g_0 can be estimated as follows:

$$g_0 = \frac{4}{3} \pi \left(\frac{m}{\rho_{\text{liq}}} \right)^2 \left(\frac{2\sigma}{k_B q \theta_{\text{max}}} \right)^3, \quad (13)$$

where θ_{max} is the supercooling parameter at the instant of nuclei injection.

According to Ref. [10], upon injection of nuclei their number (the function $v(t)$) is hardly changed; in this case, however, owing to the positive adherence–evaporation balance at the surface of the nuclei their size increases by a factor of 2–3; accordingly, the value of $x(t)$ increases by about the same factor. Due to ‘quenching’, these processes result in the production of 10^{13} – 10^{14} clusters of average size 2–4 nm (depending on the type of material). The resultant characteristic dimensions of condensed clusters as well as their size distributions are in good agreement with the experimental data of Ref. [14].

Itina and Voloshko [25] performed a highly simplified consideration of the onset of condensation in laser ablation plumes of materials and in high-power electric-discharge plasmas at atmospheric pressure. Based on separate relations of the Zel'dovich–Raizer theory in the case of thermodynamic equilibrium in the vapour, the authors obtained quite similar estimates for the size of droplet nuclei and their density at the instant of highest supercooling under comparable initial conditions – without a detailed consideration of the spatiotemporal distributions of the plasma cloud parameters, though.

The data of Refs [9–12] differ markedly from the present work as regards the initial parameters of the ablation plume (it is significantly denser and possesses a higher temperature) as well as its propagation conditions. Furthermore, also much different are the final values of the density and size of condensed particles: for lead they amount to $\sim 10^{10}$ cm⁻³ (i.e. to $\sim 10^{11}$ clusters in the plume) and to 70–80 nm, respectively [18]. In this case, the dynamics of the modelled degree of plume condensation $x(t)$ during the time interval from the instant of nuclei ‘injection’ to the instant of their ‘quenching’ are largely consistent with the data of the Anisimov–Luk’yanchuk model for vacuum. On substituting our parameters in Eqn (13) we obtain $g_0 \approx 4$ – 5 atoms (for $x = 0.1$ this corresponds to 10^{15} nuclei in the plume).

Evidently in this case the picture of condensation must be substantially different from that considered in the Anisimov–Luk’yanchuk model: during the period from the nuclei ‘injection’ to their ‘quenching’ for a smooth increase in the degree of condensation in the plume (from 0 to 0.2) there occurs a sharp (by 5–6 orders of magnitude) reduction in the number of nuclei along with the equally sharp growth of their size (the growth of linear size by two orders of magnitude corresponds to the increase in volume by six orders of magnitude). Clearly in this case it is no longer possible to attribute

the nuclei growth to only the positive balance of adherence–evaporation of the vapour atoms at the nuclei (moreover, this mechanism of droplet growth may now be neglected as being insignificant): the inclusion of coalescence of the nuclei themselves is called for. This effect has a simple physical interpretation: at the points in time close to the quenching, the external atmosphere ‘decelerates’ the leading edge of the plume, and as this takes place the inner nuclei inevitably ‘dash against’ the decelerating peripheral ones and, since the droplets are still far from solidification at that time, they readily merge into big object of regular shape.

The fact that this mechanism is quite probable is borne out by the following estimation scheme (Fig. 5). According to the previous reasoning, the production of nanoparticles terminates upon the propagation of the ‘quenching’ wave through the plume, and there occurs only their further expansion in accordance with mechanical momentum conservation law. Therefore, for the formation of a nanoparticle 70–80 nm in diameter to be possible due to only the coalescence of nuclei (without ‘attachment’ of the vapour atoms to them), the solid angle which is subtended by the cross section of the nanoparticle at the instant of ‘quenching’ termination and whose vertex is at the plume centre must contain a sufficient amount of the nuclei (i.e. $\sim 10^6$), which would run into each other in the radial rectilinear propagation to produce the nanoparticle. Since the formation of nuclei terminates upon the passage of the ‘injection’ wave, it is necessary to estimate their number in the cone subtended by the projection of the nanoparticle cross section on the plume’s front at the instant at which the ‘injection’ wave reaches the plume centre. It is readily shown that the number of nuclei that fall within such a cone is

$$N_c = \frac{xMr_{\text{part}}^2 R_q^2}{2M_0 R_c^4}, \quad (14)$$

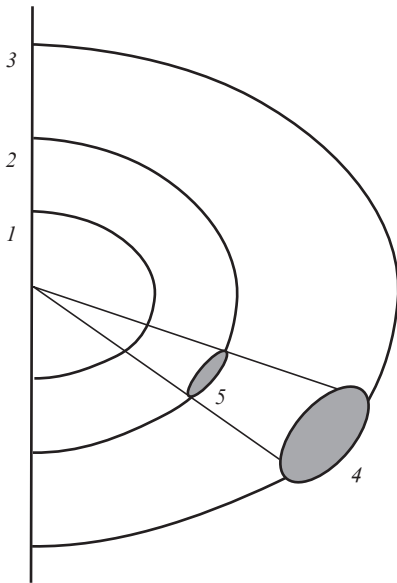


Figure 5. Scheme of estimating the number of nuclei. The plume fronts at the initial time (1) and at the instants of ‘injection’ (2) and ‘quenching’ (3) termination, as well as the resultant nanoparticle cross section (4) and the projection of the resultant nanoparticle cross section on the plume front at the instant of injection termination (5).

where r_{part} is the nanoparticle radius; R_c and R_q are the respective radii of the leading edge of the plume at the instants of ‘injection’ and ‘quenching’ termination; and M_0 is the mass of a nucleus. Substitution of the model and experimental data in formula (14) gives $N_c \approx 0.9 \times 10^6$ nuclei, i.e. the calculation strongly suggests that the most probable (and quite sufficient) mechanism of metallic nanoparticle production at the final stages of the expansion of ablation plumes at atmospheric pressure is the mechanism of ‘mass coalescence’ of the nuclei in their slowing-down by the decelerating leading edge of the plume.

Since the nuclei coalescence mechanism under description is due to the difference of pressures inside and outside the ablation plume, the following empirical relation may be suggested for describing their growth dynamics:

$$g(t) = g_0 10^\alpha, \quad \alpha = \frac{p_c p_g}{10[p_c p_g - p(t)(p_c - p_g)]}, \quad t_c < t < t_q, \quad (15)$$

where $p(t)$ is the time dependence of the pressure at the point of the plume under consideration; and p_c is the plume pressure corresponding to the instant of time t_c . This relation provides a good correspondence of the proposed model and the experimental data [18] for a broad range of metals (Pb, Zn, Ni, Cu, Ag, Au, Pt).

4. Conclusions

In the present work we have demonstrated that the Anisimov–Luk’yanchuk model can be adapted for describing the process of droplet formation in laser erosion plumes of metals at atmospheric pressure. Despite the radical difference between the practical cases considered by the authors of the model and the range of application proposed in this paper as regards the behavior of the final stage of condensation, with a certain improvement the Anisimov–Luk’yanchuk model provides, by and large, a good agreement with experimental data even without adjustment parameters. Since the type of plume expansion discussed in the present work possesses the property of self-similarity, it is possible to easily and accurately predict the development of an erosion laser plume for different initial conditions like the initial internal plume energy and the pressure of extraneous gas. This makes it possible to control rather smoothly the average size of condensed phase particles and their density. This in turn plays an important role in the development of a new avenue in technology – controlled laser-induced deposition of surface metal nanostructures at atmospheric pressure [26].

References

1. Anisimov S.I., Imas Ya.A., Romanov G.S., Khodyko Yu.V. *Deistvie lazernogo izlucheniya bol'shoi moshchnosti na metally* (Action of High Power Laser Radiation on Metals) (Moscow: Nauka, 1970).
2. Mirkin L.I. *Fizicheskie osnovy obrabotki materialov luchami lazera* (Physical Principles of Material Processing by Laser Beams) (Moscow: Izd. MGU, 1975).
3. Raizer Yu.P. *Deistvie lazernogo izlucheniya* (Action of Laser Radiation) (Moscow: Mir, 1974).
4. Prokhorov A.M., Konov V.I., Ursu I., Mikheileku I.N. *Vzaimodeistvie lazernogo izlucheniya s metallami* (Interaction of Laser Radiation with Metals) (Moscow: Nauka, 1988).
5. Rykalin N.N., Uglov A.A., Kokora A.N. *Lazernaya obrabotka materialov* (Laser Processing of Materials) (Moscow: Mashinostroenie, 1975).

6. Goncharov V.K. *Inzh.-Fiz. Zh.*, **74**, 87 (2001).
7. Sukhov L.T. *Lazernyi spektral'nyi analiz* (Laser-Assisted Spectral Analysis) (Novosibirsk: Nauka, 1990).
8. Kozadaev K.V. *Kvantovaya Elektron.*, **44**, 325 (2014) [*Quantum Electron.*, **44**, 325 (2014)].
9. Anisimov S.I., Luk'yanchuk B.S. *Usp. Fiz. Nauk*, **172**, 301 (2002) [*Phys. Usp.*, **45** (3), 293 (2002)].
10. Luk'yanchuk B.S., Marine W., Anisimov S.I., Simakina G.A. *Proc. SPIE Int. Soc. Opt. Eng.*, **3618**, 434 (1999).
11. Luk'yanchuk B.S., Marine W., Anisimov S.I. *Laser Phys.*, **8**, 291 (1998).
12. Kuwata M., Luk'yanchuk B., Yabe T. *Proc. SPIE Int. Soc. Opt. Eng.*, **4065**, 441 (2000).
13. Zel'dovich Ya.B., Raizer Yu.P. *Physics of Shock Waves and High-Temperature Hydrodynamic Phenomena* (New York: Academic Press, 1966, 1967; Moscow: Nauka, 1966) Vols 1, 2.
14. Marine W., Luk'yanchuk B., Sentis M. *Le Vide Sci. Techn., Appl.*, **288**, 440 (1998).
15. Goncharov V.K., Kozadaev K.V., Shchegrikovich D.V. *Inzhenerno-Fizicheskii Zh.*, **84**, 723 (2011).
16. Goncharov V.K., Kozadaev K.V. *Inzh.-Fiz. Zh.*, **83**, 80 (2010).
17. Goncharov V.K., Kozadaev K.V., Makarov V.V., Shchegrikovich D.V. *Inzh.-Fiz. Zh.*, **86**, 747 (2013).
18. Goncharov V.K., Kozadaev K.V., Shchegrikovich D.V. *Inzh.-Fiz. Zh.*, **86**, 754 (2013).
19. Goncharov V.K., Kozadaev K.V., Shchegrikovich D.V. *Zh. Prikl. Spektrosk.*, **80**, 409 (2013).
20. Goncharov V.K., Kozadaev K.V. *Prib. Tekh. Eksp.*, (6), 85 (2014) [*Instrum. Exp. Techniques*, **57** (6), 729 (2014)].
21. Gus'kov K.S., Gus'kov S.Yu. *Kvantovaya Elektron.*, **31**, 305 (2001) [*Quantum Electron.*, **31**, 305 (2001)].
22. Sedov L.I. *Similarity and Dimensional Methods in Mechanics* (New York: Academic Press, 1959; Moscow: Gostekhizdat, 1957).
23. Arnold N., Gruber J., Heitz J. *Appl. Phys. A*, **69**, S87 (1999).
24. Gray D.E. *American Institute of Physics Handbook* (New York: McGrawHill, 1972).
25. Itina T.E., Voloshko A. *Appl. Phys. B*, **113**, 473 (2013).
26. Kozadaev K.V. *Inzh.-Fiz. Zh.*, **87**, 682 (2014).